ISBN: 978-3-95450-214-1 ISSN: 2673-5490 doi:10.18429/JACoW-IPAC2021-THPAB219

BEAM DYNAMICS IN COHERENT ELECTRON COOLING ACCELERATOR

Yichao Jing†, Vladimir N. Litvinenko[1], Igor Pinayev, Yuanhui Wu[1]
Collider-Accelerator Department, Brookhaven National Laboratory, Upton, NY, USA
Irina Petrushina, Kai Shih
Physics Department, Stony Brook University, NY, USA
[1]also at Physics Department, Stony Brook University, NY, USA

Abstract

The ongoing Coherent electron Cooling (CeC) proof-of-principal project requires a high quality electron beam to be generated, compressed and propagated through the beam line. A start to end accelerator design with consideration of space charge effect, wakefields and nonlinear dynamics such as coherent synchrotron radiation and chromatic aberration was performed in generating such high brightness electron beam. In this paper, we present our recent study on the beam dynamics of such beam and compare with what was measured in experiment.

INTRODUCTION

The CeC beamline (Fig. 1) consists of low energy beam transport (where electron beam is prepared and accelerated to a total energy of 14.56 MeV), a dogleg section to transport the beam to a common section where the electron beam is co-propagating with the hadron beam. In the common section, the electron beam is matched to beam requirements in cooling section where the electron beam co-propagates with the hadron beam.

The performance of the cooling is highly dependent on the electron beam's quality. Thus a self-consistent start to end (S2E) simulation of the accelerator section is crucial in determining the amplifier's performance and in predicting the machine setups to characterize the cooling.

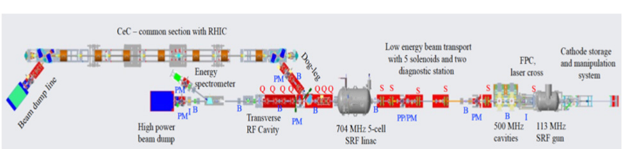

Figure 1: Engineering drawing of CeC beamline (electron beam travels from right to left).

LOW ENERGY BEAM DYNAMICS

There are three RF systems in the CeC's accelerator section – a quarter-wave SRF gun cavity (1.25 MeV, 113 MHz), a NC bunching cavities (tunable for different peak current, usually at about 160 to 180 keV, 500 MHz) and a 5-cell SRF linac (13.1 MeV, 704 MHz). All three RF systems are operated at harmonics of a global clock, 78 kHz – the RHIC's revolution frequency. In between cavities, 6 solenoids are used for electron beam's phase space manipulation and beam size control. More specifically, the solenoid in between gun cavity and the linac is used to perform emittance compensation, i.e., provide optimal transverse focusing to minimize emittance growth from space charge effect of low energy electron beam, which is illustrated in Fig. 2. After the beam gains energy chirp from bunching cavities and experiences ballistic compression in long straight section (~ 10 m to linac), the beam current increases to ~ 50 – 100 amps prior to entrance into linac where the space charge effect is dominating. In additional, we alternate the polarity of the 5 solenoids in this 10-m long drift to control any systematic field errors and maintain the initial coordinate systems so that the lowest order chromatic effect introduced by misalignments in magnets is compensated. The beam size is focused and matched to optimal beam conditions at the entrance of the linac.

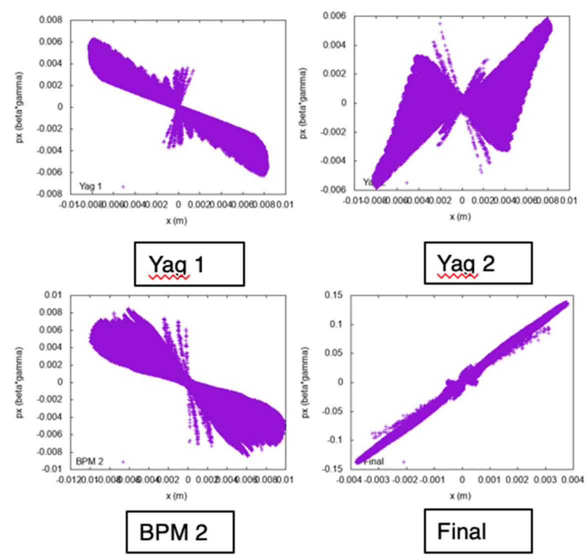

Figure 2: Solenoidal fields were adjusted and optimized in the low energy beam transport so that at the end of the beam line, all longitudinal slices along the beam are aligned in the phase space to reduce the projected emittance.

There are many different beam dynamics in the beam line that could potentially affect beam qualities severely, namely space charge, wakefields, shielding effect from vaccum chamber etc. Doing all beam dynamics in one simulation code is unimaginable. We used many dedicated codes to calculate these effects before importing the simulated results into the IMPACT-T [1] to track particles' 6D evolution along the beamline. We benchmarked our

† yjing@bnl.gov

ISBN: 978-3-95450-214-1 ISSN: 2673-5490 doi:10.18429/JACoW-IPAC2021-THPAB219

calculated beam properties (like beam envelope, phase space distributions, energy evolutions) in IMPACT-T with many other well established beam dynamics codes e.g., GPT/PARMELA/ASTRA.

We recessed our cathode position in the gun cavity so that the initial RF field provides a strong transverse focusing to the beam. With adjusted cathode recess position, the proper focusing force can be selected to better suit beam dynamics in the gun [2].

As mentioned above, we used a bunching cavity to provide energy chirp in the low energy beam (~ 1.25 MeV kinetic energy) for the beam to undergo a ballistic compression in the long beam transport prior to getting a major boost in energy in the 704 cavity (~ 13.1 MeV kinetic energy gain). The energy distribution in different beam slices will have different rotation in solenoids which are used to provide focusing. Such process smears out the transverse phase space and by carefully tuning up the solenoids, the longitudinal slices along the beam are aligned in the phase space to reduce the projected emittance at the end of the low energy beam line. Detailed plots of the transverse phase space evolution can be visualized from particle tracking in IMPACT-T shown in Fig. 2.

Optimization in IMPACT-T takes all beam line components as variables (magnets, cavities…). The optimization goals were to achieve high peak current for core part of the beam while keep the overall as well as sliced emittances low. Figure 3 shows the longitudinal phase space of electron beam at the end of linac (@ 13.6 meters from cathode). For a beam with bunch charge 1.5 nC, the peak current of the beam is compressed more than 25 fold reaching 75 A after the low energy line and sliced energy spread after linac is lower than 2e-4.

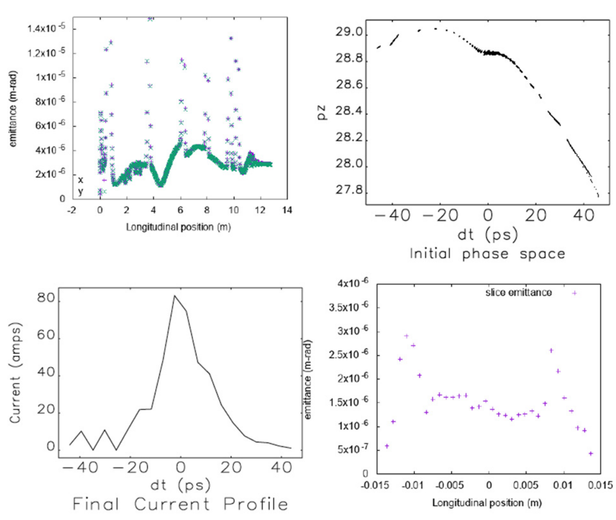

Figure 3: The electron beam at the end of linac reaches very high 6D brightness: transverse emittances (projected) less than 4 um while sliced emittances are lower than 1.5 um for core, peak current higher than 75 A and sliced fractional energy spread is less than 2e-4.

BENCHMARK WITH EXPERIMENT

The achieved beam properties at the end of the accelerator section proves a newly achieved high brightness beam for space charge dominated beam, especially for which undergoes beyond 20-fold compression in the beam current.

To verify what we achieved in simulation experimentally, we benchmarked our findings in IMPACT-T of the evolution of beam envelope, emittance, energy, bunch-length, etc, with measurements using diagnostics implemented through the beamline. A beam image on one of the YAG profile monitors can be seen in Fig. 4.

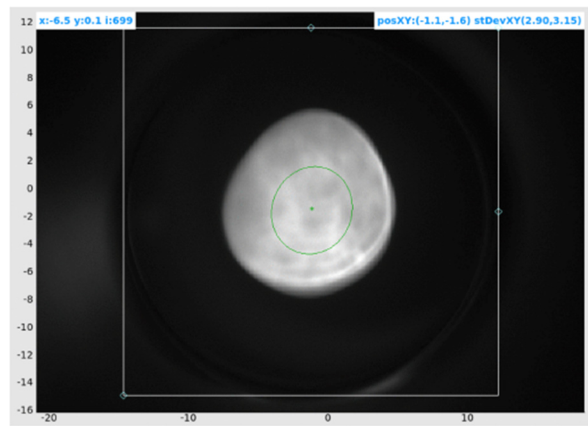

Figure 4: Beam image taken after buncher cavity on a YAG profile monitor. Beam size, position and distributions are extracted and compared with simulation.

Using the multi-stage beam diagnostics, including yags, bpms, pepperpot etc (details can be found in Fig. 1), we can benchmark our simulation results with experiment and thus gain better understanding of our physics models and possible missing factors in the simulation setup.

As shown in Fig. 5, in one of the dedicated benchmark experiments, where we scanned couple of solenoids in the beamline and measured beam size dependence downstream, which to be compared with simulation predictions. The agreement is excellent.

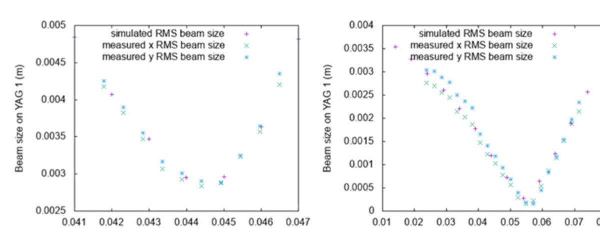

Figure 5: Measured beam sizes dependence on SRF solenoid and one of the LEBT solenoids have very good agreement with simulated envelopes.

ISBN: 978-3-95450-214-1 ISSN: 2673-5490 doi:10.18429/JACoW-IPAC2021-THPAB219

Another dedicated benchmark experiments to compare longitudinal phase space can be found in Fig. 6. We obtained the beam image on one of our profile monitor in dispersive section of the beam line (namely, a dogleg) and extracted the beam information from such image. Our simulation's prediction has very good agreement with what was obtained. In the current calendar year, we have a newly installed diagnostic beam line, where a more direct measurement of longitudinal phase space can be achieved with implementation of a transverse deflecting cavity.

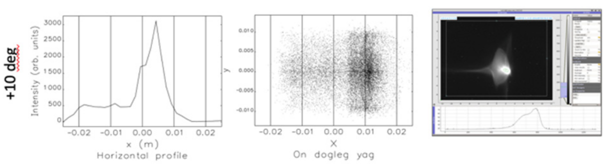

Figure 6: Comparison of beam longitudinal profile with shifted linac phase on profile monitor in dispersive region has very close resemblance with simulation prediction.

LOW BEAM NOISE STUDY

With the confidence of our understanding of important beam dynamics existing in the electron beam and the capability of precisely predicting such beam's properties and performance. We set up a lengthy simulation to further investigate micro-structures resides inside the electron beam.

It is well known that in a strongly focused lattice (to overcome strong space charge), the electron beam distribution could develop some longitudinal instabilities, i.e., micro-bunching instabilities. Such instabilities, having close dependence on the initial beam noise and usually amplifying the former, would adversely affect the cooling performance. In other words, we need to develop a lattice that has no amplification of initial noises while provides a high performance channel for beam propagation. With careful study and comparison of different beam line setups, we made sure that our low energy beam transport has no amplification on any of the initial beam noises that might resides in the beam. Figure 7 shows a plot of the FFT of beam longitudinal distribution at the end of two different beam lines which generate similar final electron beam properties. The spectrum on the left has an obvious hump at around 10 THz which overlaps with one of the cooling frequency thus could not be used. The lattice on the right, on the other hand, has no frequency response apart from the zero frequency which decays exponentially and represents the poisson distribution of a compressed electron bunch. The sharp spikes are correlated to the computation domain size in simulation and thus are artificial.

After the linac, we used 8 quadrupoles (3 after linac, 1 in the middle of dogleg and 4 before the undulator) to match the beam optics from the exit of low energy beam transport (LEBT) to the entrance of FEL (2 quads in dogleg are fixed for dispersion matching). Alternating quadrupole settings are implemented to minimize the beam size along the beam line. Figure 8 shows the beam envelop calculated in ELEGANT [3] using the particle distribution from our start to end particle-in-cell tracking code.

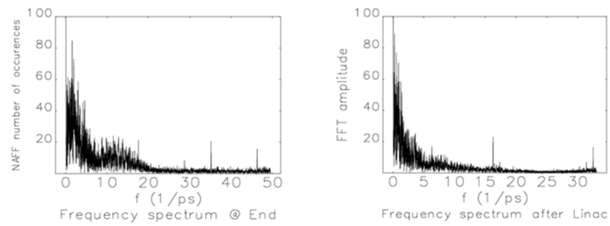

Figure 7: Optics matching from the end of LEBT to and along the FEL section was done in ELEGANT using alternating quadrupoles.

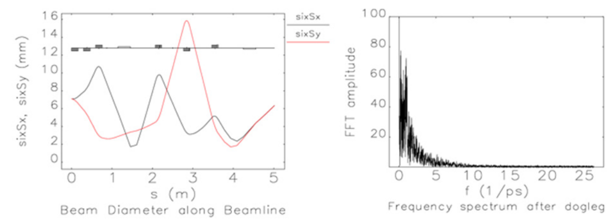

Figure 8: Beam emittance can be blown up when the energy spread is large (~ 1%, right). The emittance growth in dogleg is minimal while energy spread is reasonably low (~ 0.1%, left).

The spectrum of the longitudinal beam distribution shows a structure developed after the dogleg at around 1 THz. We performed a dedicated synchrotron radiation simulation in SRW and verifies that such structure comes from synchrotron radiation in the dipoles. It is, however, located outside of our interested regime of spectrum thus causes no hazard to the cooling performance.

CONCLUSION

We designed and performed the S2E simulation in a space charge dominated beam and studied various beam dynamics issues. The beam properties are optimized while longitudinal beam size is compressed by more than 20 fold. We demonstrated the high beam brightness and low beam noise for this beam experimentally.

Work is supported by Brookhaven Science Associates, LLC under Contract No. DEAC0298-CH10886 with the U.S. Department of Energy, DOE NP office grant DEFOA-0000632, and NSF grant PHY-1415252.

REFERENCES

[1] Ji Qiang, IMPACT-T A 3D Parallel Particle Tracking Code in Time Domain, https://amac.lbl.gov/~jiqiang/IMPACT-T/index.html

[2] I. Petrushina *et al.*, "Superconducting RF Gun With High Current and the Capability to Generate Polarized Electron Beams", presented at the 12th Int. Particle Accelerator Conf. (IPAC'21), Campinas, Brazil, May 2021, paper WEPAB138.

[3] M. Borland, "ELEGANT: A flexible SDDS-compliant code for accelerator simulation", ANL, IL, USA, Rep. LS-287, Aug. 2000. doi:10.2172/761286